

Radiofluorescence of quartz from rocks and sediments and its correlation with thermoluminescence and optically stimulated luminescence sensitivities

Pontien Niyonzima^{1*}, André O. Sawakuchi¹, Mayank Jain², Raju Kumar², Thays D. Mineli¹, Ian del Río¹ and Fabiano N. Pupim^{1,3}

¹ Luminescence and Gamma Spectrometry Laboratory (LEGaL), Instituto de Geociências, Universidade de São Paulo, São Paulo, Rua do Lago 562, São Paulo, SP 05508-080, Brazil

² Department of Physics, Technical University of Denmark, DTU Risø Campus, DK-4000 Roskilde, Denmark

³ Departamento de Ciências Ambientais, Universidade Federal de São Paulo, Diadema, Rua São Nicolau, 210, São Paulo 09913-030, Brazil

*Corresponding Author: pontienn@usp.br

Received: May 22, 2020; in final form: June 18, 2020

Abstract

The present study examines radiofluorescence (RF) emissions in quartz from parent rocks (igneous plutonic and volcanic) and sediments of different provenances, which represent a range of optically stimulated luminescence (OSL) and thermoluminescence (TL) sensitivities observed in nature. OSL and TL (110 °C peak) sensitivities of quartz have been successfully used for sediment provenance analysis, but the considerable sensitivity variations are still poorly understood in terms of charge traps and recombination centers. In the studied samples, the RF spectra obtained at room temperature and using X-ray irradiation consist of two broad emission bands: the first emission band is centered at ~1.9 eV (blue) and has a higher intensity compared to the second emission band centered at ~3.5 eV (ultraviolet, UV). The deconvolution analysis confirms that the quartz RF spectrum is at least the sum of four emission bands located between 1.5 eV (827 nm) and 4.0 eV (310 nm). The general observation is that the RF intensity differs between quartz from rocks and sediments, and among quartz from sediments with different provenances. Generally, quartz from sediments showed higher RF intensity compared to quartz from rocks, rendering the same pattern observed for OSL and TL sensitivities. For quartz from sediments, we ob-

served strong correlations between the UV-RF band intensity and the OSL or 110 °C TL sensitivities. We argue that these correlations may be attributed to the fact that both 110 °C TL peak and OSL of quartz use the same recombination centers rather than the same electron trap. The UV-RF intensity measured using X-ray sources can also be used for provenance analysis of sediments in the same way as the OSL and TL sensitivities.

Keywords: Quartz in sediments, Sediment provenance, Luminescence of quartz, Radiofluorescence spectra, X-ray irradiation

1. Introduction

Since the first proposals for the use of thermoluminescence (TL) (e.g., Grögler et al. 1958; Fleming 1970; Mejdahl 1979; Wintle & Huntley 1979) and optically stimulated luminescence (OSL) in quartz (Huntley et al., 1985) as dating techniques, it appears that both TL and OSL signals are not merely due to charge eviction from traps after stimulation with consequent luminescence recombination. However, more complex mechanisms are involved (Martini et al., 2009). Aitken & Smith (1988) reported parallel changes in the OSL sensitivity and the sensitivity of the 110 °C TL peak and suggested that this might be related to a common mechanism. Most researchers agree on the involvement of the same recombination centers of these two processes (e.g.,

Table 1. Description of studied samples, indicating types of rocks and sediments, approximate age of crystallization (rocks) or deposition (sediments), location of the sampling sites, and average TL and OSL sensitivities and standard deviation as presented in unpublished work by Mineli et al. Aliquots used to measure TL, and OSL sensitivities contained approximately 150 to 200 grains, as observed under an optical microscope, with an average mass of 8.1 ± 0.9 mg. TL and OSL sensitivities data were not obtained for sample L0680, which was collected in the same geological setting of sample L0674. Both samples are examples of sediments with low sensitivity quartz. For both TL and OSL measurements, 2 to 6 aliquots were measured for each sample and results presented in the table are average with standard.

	Code	Name	Age	Location	TL 110 °C (cts Gy ⁻¹)	OSL (cts Gy ⁻¹)
Rocks	VR12	Granite	Neoproterozoic	Ribeira Fold Belt, Guaraú Massif, (Cajati, São Paulo, Brazil)	1865 ± 1851	67 ± 70
	ITA1	Granite	Neoproterozoic	Ribeira Fold Belt, Itacoatiara Massif, (Niterói, Rio de Janeiro, Brazil)	2019 ± 261	4.4
	LA1	Rhyolite	Pleistocene	Los Alamos (New Mexico, USA)	1795 ± 319	63 ± 25
	IP22	Hydro-thermal quartz	Permian	Teresina Formation, Paraná Basin (Anhembi, São Paulo, Brazil)	108	2.2
Sediments	L0001	Coastal sand	Pleistocene	South Atlantic Coast (Southern Brazil)	128760 ± 42674	23152 ± 9361
	L0017	Fluvial sand	Pleistocene	Central Amazon (Northern Brazil)	22426 ± 5354	1390 ± 502
	L0698	Fluvial sand	Holocene	Western Amazon (Northern Brazil)	12396 ± 4036	2432 ± 1309
	L0229	Fluvial sand	Pleistocene	Pantanal Wetland (Western Brazil)	308683 ± 51341	53520 ± 9522
	L0688	Fluvial sand	Holocene	Paraná River Basin (Southern Brazil)	433092 ± 53278	89544 ± 53278
	L0572	Fluvial sand	Pleistocene	Central Amazon (Northern Brazil)		
	L0674	Alluvial sand	Pleistocene	Mejillones Peninsula, Andes (Chile)	266 ± 44	17 ± 9
	L0680	Colluvial sand	Pleistocene	Salar Del Carmen, Andes (Chile)	*	*

Chen et al. 2000). Radiofluorescence (RF), the light emission during irradiation, has been investigated in quartz samples from rocks and sediments as well as in artificially growing SiO₂ crystals (Marazuev et al., 1995; Krbetschek & Trautmann, 2000; Martini et al., 2012b) for dosimetry and dating purposes. RF has also been investigated for a better understanding of the luminescence dynamics in quartz (Martini et al., 2012a,b; Chithambo & Niyonzima, 2017) by compar-

ing the 3.44 eV RF peak intensity measured after series of irradiation and thermal treatments in order to understand the specific role of various defect centers. Different from TL and OSL, the RF emission seems to correspond predominantly to the direct recombination of electrons from the conduction band with the holes at the recombination centers during irradiation (e.g., Schmidt et al. 2015; Friedrich et al. 2017).

Deconvolution of the RF spectra showed the presence

of the same emission bands from both natural and “artificial” (laboratory crystal growth) quartz crystals, indicating that the same luminescence processes are involved (Martini et al., 2012a,b; Chithambo & Niyonzima, 2017). The similarity among RF, TL and OSL emission spectra (Huntley et al., 1991; Krbetschek et al., 1997; Schilles et al., 2001) provided evidence that these luminescence signals share the same recombination centers (Friedrich et al., 2017). This similarity suggests that changes in OSL and TL sensitivities in nature, as observed in quartz from sediments (e.g., Pietsch et al. 2008; Zular et al. 2015) are probably related to the recombination process rather than trapping process. In this way, investigation of the relationship between RF and OSL and TL sensitivities can shed light on the role of recombination centers for the natural sensitization processes. In addition to its widespread application for dating of Quaternary sediments (Aitken, 1998), luminescence signals from quartz are used for tracing the provenance of sediments (e.g., Lü & Sun 2011, Gray et al. 2019). In the previous works, TL spectra (Rink et al., 1993), the proportion of OSL components (Tsukamoto et al., 2011), the OSL and TL sensitivities (Sawakuchi et al., 2012; Zular et al., 2015; Mendes et al., 2019) and OSL signal components (Nian et al., 2019) of quartz have been used in discriminating sediment sources and provenance analysis. Thus, several luminescence properties (e.g., sensitivity, thermal activation, spectral variation, and signal components) can be used to discriminate quartz from different provenances. A general pattern is that quartz extracted from different types of igneous and metamorphic rocks has a relatively low luminescence sensitivity (Chithambo et al., 2007; Guralnik et al., 2015) compared to quartz from sediments, which shows a wide range of OSL sensitivity variation (Sawakuchi et al., 2011). Thus, recent studies have successfully applied OSL sensitivity in sediment provenance analysis through discrimination of sediments with different transport histories since their parent rocks (e.g., Sawakuchi et al. 2018; Mendes et al. 2019).

In this study, we investigate the variation of RF emission spectra in quartz extracted from different igneous rocks, which are primary sources of terrigenous sediments, and sediments of different geological settings, ranging from tectonic active mountain ranges to stable craton areas in South America. This suite of samples has a broad range in natural TL and OSL sensitivities, as presented in Sawakuchi et al. (2020) and unpublished work by Mineli et al. and summarized in Table 1. Correlation between UV-RF and sensitivity of both TL and OSL is also investigated in this study. We hypothesize that, this correlation would support the use of RF of quartz for sediment provenance analysis.

2. Experimental details

2.1. Sample description and preparation

Samples used in this investigation were quartz from igneous rocks (granite, rhyolite, and hydrothermal vein) representing different conditions of quartz crystallization and sed-

Step	OSL and TL sensitivities ^a
1	Bleach with blue LEDs at 125 °C for 100 s
2	Dose: 10 Gy
3	TL up to 190 °C (5 °C/s) (110 °C TL sensitivity)
4	Blue stimulation at 125 °C for 100 s (OSL sensitivity)
5	Blue stimulation at 125 °C for 100 s (background)

Table 2. Measurement protocol used by Mineli et al. (pers. comm.) for determination of TL (step 3) and OSL (step 4) sensitivities. The 110 °C TL sensitivity was determined through the integration of the 75–125 °C interval of the TL glow curve and the OSL sensitivity through the first second of light emission of the OSL decay curve

iments (alluvial, fluvial and coastal sands) of different depositional environments from South American sites (Table 1). OSL and TL sensitivities of these samples were previously studied by Mineli et al. (pers. comm.) and they are summarized in Table 1.

Rock samples were crushed to release quartz crystals, which were manually picked for careful grinding using a pestle and ceramic mortar. Quartz crystals from igneous rocks and quartz grains from sediments in the range of 180–250 µm were extracted by wet sieving. The target fraction was treated with hydrogen peroxide (H₂O₂, 27%) and hydrochloric acid (HCl, 10%) to remove organic matter and carbonate minerals, respectively. Heavy minerals and feldspar grains were removed by heavy liquid separation with lithium metatungstate solutions with densities of 2.75 g/cm³ and 2.62 g/cm³, respectively. To purify and concentrate the quartz fraction, samples were etched in 38% hydrofluoric acid (HF) for 40 min. Infrared stimulation (IR) was performed to confirm the absence of feldspar contamination in the HF treated quartz fraction. Samples with remaining feldspar were subjected to steps of HF 5% etching for 24 hours followed by wet sieving (180 µm sieve), and in some cases, samples were repeatedly HF-etched until a negligible infrared signal was achieved, compared with blue stimulation signal.

2.2. Instrumentation

Radiofluorescence measurements were carried out using the Risø station for Cryogenic Luminescence Research COLUR at Center for Nuclear Technologies, Technical University of Denmark (DTU), Risø campus. It consists of a Horiba Fluorolog-3 spectrometer expanded to include multi-excitation and detection ports, an X-ray irradiator (40 kV anode voltage, 100 µA anode current, and ca 0.06 Gy/s dose rate to quartz), and a temperature-controlled closed-loop He cryostat (7–300 K) (Prasad et al., 2016).

All the radiofluorescence measurements reported in this paper were obtained using X-ray irradiation at room temperature and a CCD detector. Quartz grains were mounted on a steel cup using double-sided tape. Measurements were performed with a constant dose rate (ca 0.06 Gy/s), integration

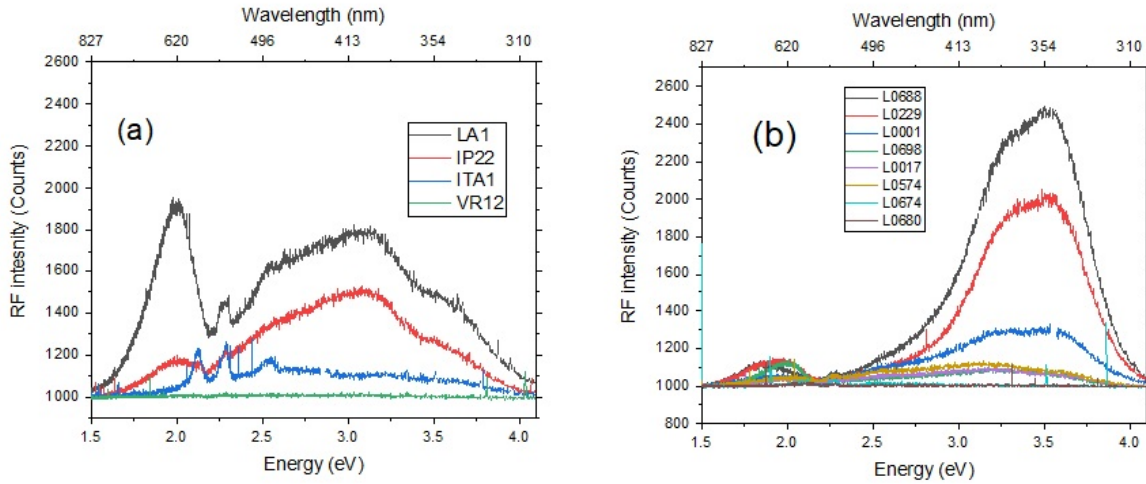


Figure 1. Comparison of the RF emission spectra measured in quartz from rocks (a) and sediments (b).

times of 30 s (~ 1.8 Gy) for quartz sediment grains (samples L0001, L0017, L0229, L0572, L0674, L0680, L0688, and L0698) and 300 s (~ 18 Gy) for quartz rock crystals (samples VR12, ITA1, LA1, and IP22) and full-range detection (300-1,000 nm). Integration times were higher for quartz from rocks to acquire significant RF spectra. Background emission was acquired by measuring empty cups with tape. Samples were exposed to daylight, but they were not submitted to any thermal or irradiation treatment before the acquisition of RF spectra. RF spectra were deconvoluted into Gaussian components using the least square method with the Levenberg-Marquardt algorithm (Origin software 2018).

The same quartz samples used for RF measurements were previously submitted to OSL and TL sensitivity measurements performed in the two Risø TL/OSL DA-20 readers at the Luminescence and Gamma Spectrometry Laboratory (LEGaL) of the Institute of Geosciences, University of São Paulo, Brazil. The OSL and TL sensitivity data are summarized in Table 1. The measurement protocol is described in Table 1. Aliquots of similar masses were used in order to minimize the effect of aliquot size on luminescence signal sensitivity. The readers are equipped with a beta-radiation source ($^{90}\text{Sr}/^{90}\text{Y}$) with dose rates of ca 0.132 Gy/s and ca

0.077 Gy/s, blue (470 nm, max. 80 mW cm⁻²) and infrared (870 nm, max. 145 mW cm⁻²) LEDs for stimulation and Hoya U-340 filters (200–400 nm) for light detection in the ultraviolet band. Regarding the instrument response spectra correction, RF and OSL/TL measurements were done on different equipment, and the absolute counts of RF and OSL sensitivities are not directly comparable. However, the main goal of this study is the relative comparison between RF and OSL/TL. In the TL and OSL measurements carried out by Mineli et al. (pers. comm.), quartz aliquots were mounted on 9.7 mm diameter stainless steel discs using silicone oil. Each aliquot contained approximately 150 to 200 grains, as observed under an optical microscope, with an average mass of 8.1 ± 0.9 mg (see procedures for aliquot preparation in Mendes et al. (2019)).

3. Results

The comparison between RF spectra of quartz from rocks and sediments is shown in Figure 1. Both types of quartz show similar RF in higher energy part of the spectrum (2.5–4.0 eV), despite the difference in their intensities and number of overlapping peaks, while in the lower part of the spectrum

Bands	Sediment sample L0688		Rock sample LA1	
	Energy (eV)	FWHM (eV)	Energy (eV)	FWHM (eV)
Peak 1	1.87	0.32	1.97	0.34
Peak 2	2.55	0.99	2.53	0.48
Peak 3	3.36	0.37	3.07	0.71
Peak 4	3.62	0.42	3.70	0.49

Table 3. Energy values of the detected emission bands for quartz from rock (LA1) and sediment (L0688) samples.

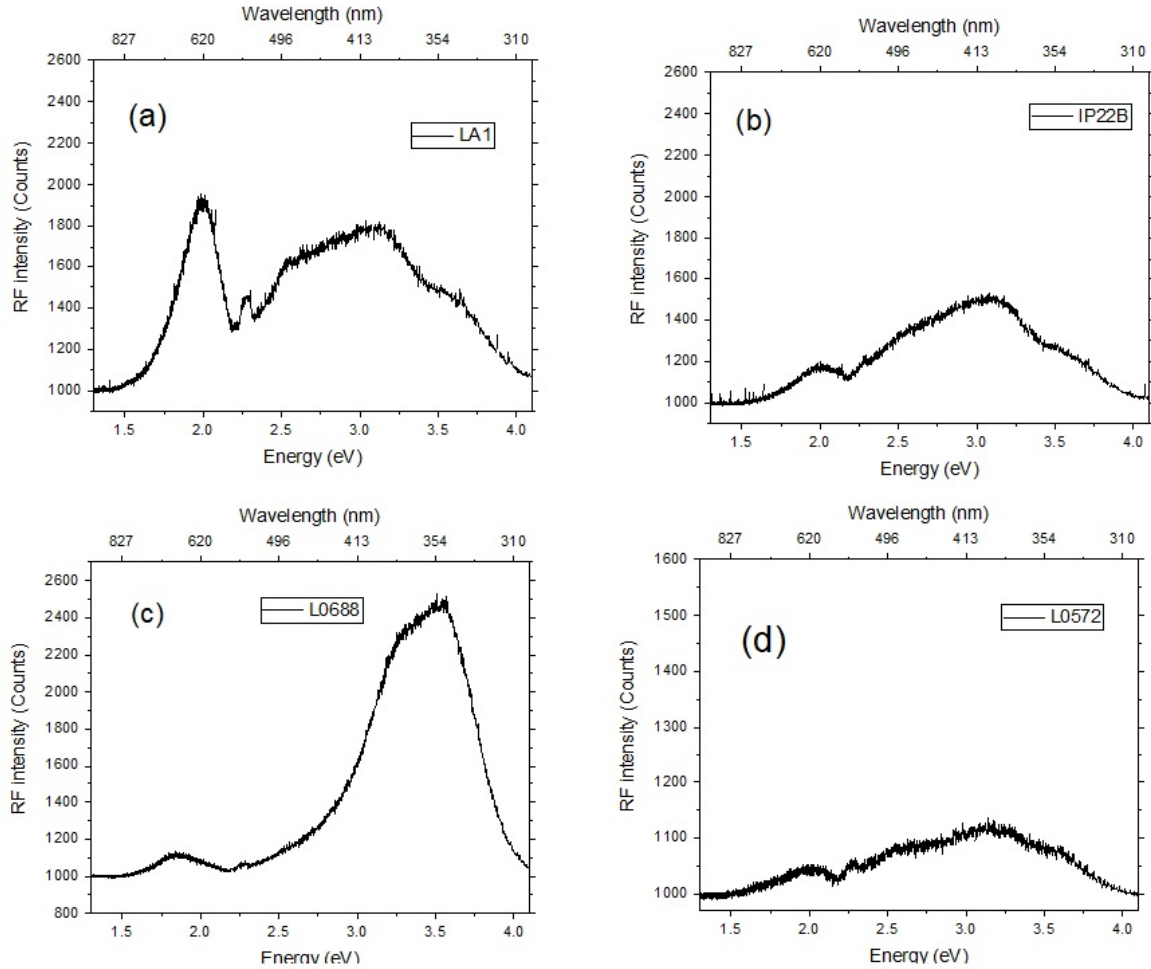


Figure 2. Spectra to illustrate the differences in RF intensities for quartz from rocks and sediments. RF spectra of quartz from rhyolite (a) and hydrothermal vein (b) have relatively low RF intensity compared to quartz from sediments of stable tectonic areas in southern Brazil (c). However, quartz from sediments of the Chilean Andes (d) has low RF intensity, comparable to quartz from rocks. The sample description can be found in Table 1.

(1.5–2.5 eV), non-similarity in the RF spectra was observed.

The luminescence spectra of quartz samples used in this study showed a broad unstructured emission ranging from 1.5 eV (827 nm) to 4.1 eV (310 nm), with maximum RF intensity close to 2.0 eV (620 nm) for quartz from rocks (Figure 1a) and 3.6 eV (354 nm) for quartz from sediments (Figure 1b). For the emission spectra of quartz from rocks (Figure 1a), we identified five different emission bands represented by a broader band in the range of 1.6–2.1 eV (red), a narrow emission band centered at 2.3 eV and bands at 2.4–2.8 eV (blue), 3.0–3.4 eV (UV-violet) and 3.4–3.8 eV (UV). The visual analysis of the emission spectra of quartz from sediments resulted in the identification of four different emissions at 1.6–2.2 eV (red), around 2.3–2.7 eV (blue), 3.0–3.3 eV (UV-violet) and 3.5–3.8 eV (UV) (Figure 1b). The RF intensity in some samples was not strong enough to perform a curve fitting analysis (Figure 1).

Generally, quartz from sediments of central and southern Brazil, represented by samples from the Paraná River

(L0688), Southern Atlantic coast (L0001) and Pantanal Wetland (L0229), showed high UV-RF emission intensity compared to sediments from Chilean Andes, i.e., Mejillones Peninsula (L0674) and Salar Del Carmen (L0680). For quartz from Brazilian sediments, the exceptions are the samples from northern Brazil, i.e., central Amazon (L0572) and western Amazon (L0017 and L0698), that showed low RF intensity compared to that of quartz from central and southern Brazil used in this study. For the samples from rocks, quartz from granite (VR12 and ITA1) shows low RF intensity compared to quartz from rhyolite (LA1) and hydrothermal vein (IP22). Figure 2 shows the main characteristics of RF spectra recorded for quartz from rocks (LA1 and IP22) and sediments with higher (L0688) and lower (L0572) RF intensities.

All the RF emission spectra from quartz extracted from both rocks and sediments have been deconvoluted into their main components (Figure 3). The fitting of the RF emission spectra was performed assuming four bands, and the Gaus-

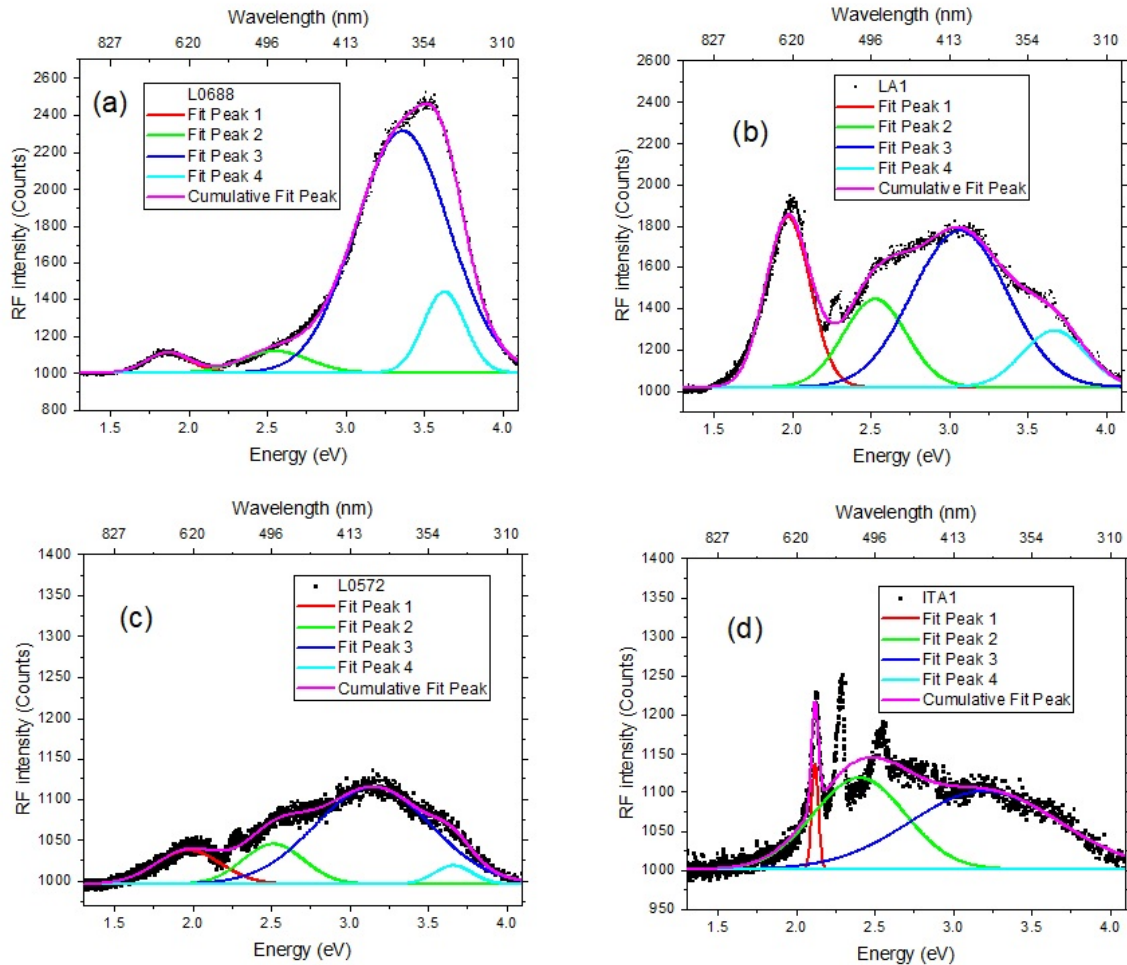


Figure 3. Gaussian components of high-intensity RF emission spectra of quartz from sediments of the Paraná River Basin (a) and rhyolite of Los Alamos (b). Gaussian components of low-intensity RF emission spectra of quartz from sediments of Central Amazon (c) and granite of the Ribeira Fold Belt (d).

sian fitting agrees with experimental curves for samples with high RF intensity (Figure 3a).

The energy and full width at half-maximum for the four emission bands used in the deconvolution of the RF spectra are presented in Table 1, i.e., 1.87 eV (0.32 eV), 2.55 eV (0.99 eV), 3.36 eV (0.37 eV), 3.62 eV (0.42 eV) for quartz from sediments (L0688) and 1.97 eV (0.34 eV), 2.53 eV (0.48 eV), 3.07 eV (0.71 eV) and 3.7 eV (0.49 eV) for quartz from rocks (LA1). [Martini et al. \(2012b\)](#) reported five emission bands in natural quartz, i.e., 1.95 eV (0.48 eV), 2.53 eV (0.46 eV), 2.80 eV (0.45 eV), 3.44 eV (0.58 eV) and 3.94 eV (0.49 eV). Values within brackets are full width at half-maximum of the emission bands. More studies are needed to investigate the reasons behind the difference in the number of RF emission bands and values of their full width at half-maximum for quartz from Brazil and quartz from other regions.

For the quartz from rocks and quartz from sediment samples (e.g., L0572, Figure 3c) with low RF intensity, Gaussian fittings are not entirely satisfactory in the energy region rang-

ing from 2.1 eV to 2.4 eV (Figure 3b, c, and d), where small and sharp peaks might be sample related or instrumental artifacts. Other candidates to explain the presence of these sharp peaks are the presence of other mineral phases as inclusions in quartz, such as zircon or apatite. However, additional mineral inclusion analysis is required to confirm or reject this statement.

Bands with peaks at 3.36 eV and 3.6 eV are the most intense in the sediment samples, and a band with a peak at 1.9 eV is the most intense for rock samples. Bands with peaks at 2.5 eV, 3.07 eV, and 3.7 eV are overlapping, as observed in quartz from rhyolite (Figure 3b). The RF intensities of bands with peaks at 3.07 eV and 3.70 eV for quartz from rocks and at 3.36 eV and 3.62 eV for quartz from sediments were used to investigate the relationship between UV-RF and the sensitivities of the 110 °C TL peak and OSL (initial 1 s of light emission) assessed by [Mineli et al. \(pers. comm.\)](#) (Figure 4).

A linear correlation, with a correlation coefficient (r) ranging from 0.95 to 0.99, between UV-RF and the sensitivities of the 110 °C TL peak, and the OSL (first 1s) is observed

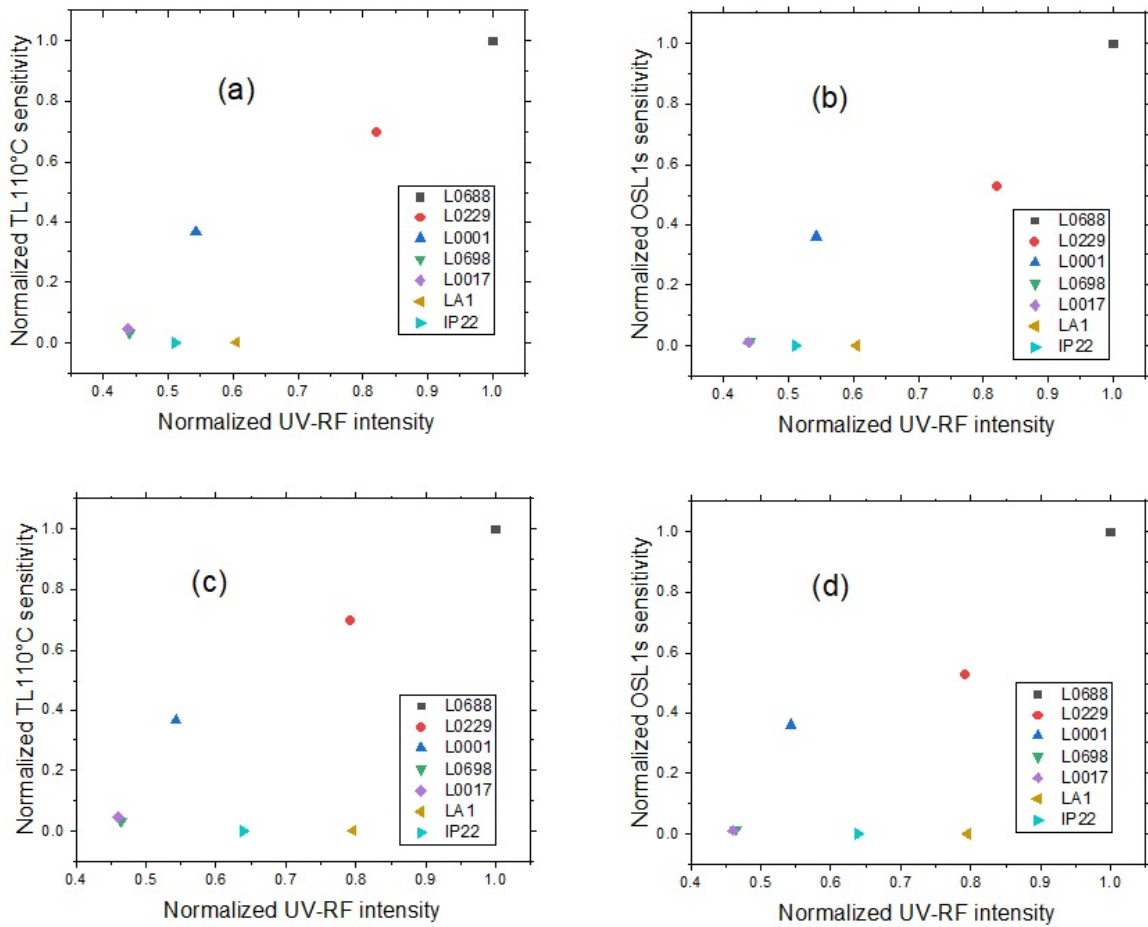


Figure 4. Relationship between 3.6 eV RF emission band intensity and sensitivities of 110 °C TL peak (a) and OSL (b); and between 3.36 eV RF emission band intensity and sensitivities of 110 °C TL peak (c) and OSL (d). The sensitivity of the OSL signal was taken from the integral of the initial second of the OSL decay curve divided by the given radiation dose. The sensitivity of the 110 °C TL peak (heating rate of 5°C/s) was determined from the integration of the 75–125 °C interval divided by the given dose. The TL and OSL sensitivities and UV-RF intensity were normalized to their corresponding highest signal for easy comparison.

for quartz extracted from sediments (Figure 5). However, no correlation was observed for quartz from rocks (LA1 and IP22) (Figure 4). The results from Figure 5 indicate that samples with high UV-RF intensity are more sensitive in the case of both 110 °C TL and OSL (first 1s).

4. Discussion and conclusions

In quartz, the correlation between the sensitivities of the 110 °C TL peak and the first 1s of the OSL decay curve has been widely acknowledged, indicating that the fast OSL component and 110 °C TL peak sensitize in a similar manner (Jain et al., 2003). In this study, we present the correlation between both OSL and TL sensitivities with RF intensity of quartz from sediments, which support the use of RF as provenance proxy in the same way as OSL and TL sensitivities.

The RF and TL emissions were found to be similar in the violet, blue, and red regions, suggesting that their recombi-

nation centers must be closely related to each other (Shimizu et al., 2006). According to Huntley et al. (1991), the OSL spectra of quartz have been observed in the ultraviolet region, so that the UV-RF (3.6 eV and 3.36 eV) emissions might also be related to the UV-OSL emission. In this study, we observed a linear correlation between the OSL sensitivity, presumably dominated by the fast component, and UV-RF (3.6 eV and 3.36 eV) intensity for quartz from sediments. We also observed a linear correlation between UV-RF and sensitivity of 110 °C TL, which strongly supports the suggestion that sensitization processes in nature might be due to changes in recombination process (density of recombination centers for example) rather than changes in the charge trapping probability like proposed by Moska & Murray (2006).

In the present work, we also observe low RF intensity of quartz from rocks compared to quartz from sediments, which is a pattern also observed for the OSL sensitivity of quartz (Sawakuchi et al., 2011). The RF sensitization, when quartz is released from parent rocks to sedimentary systems, occurs

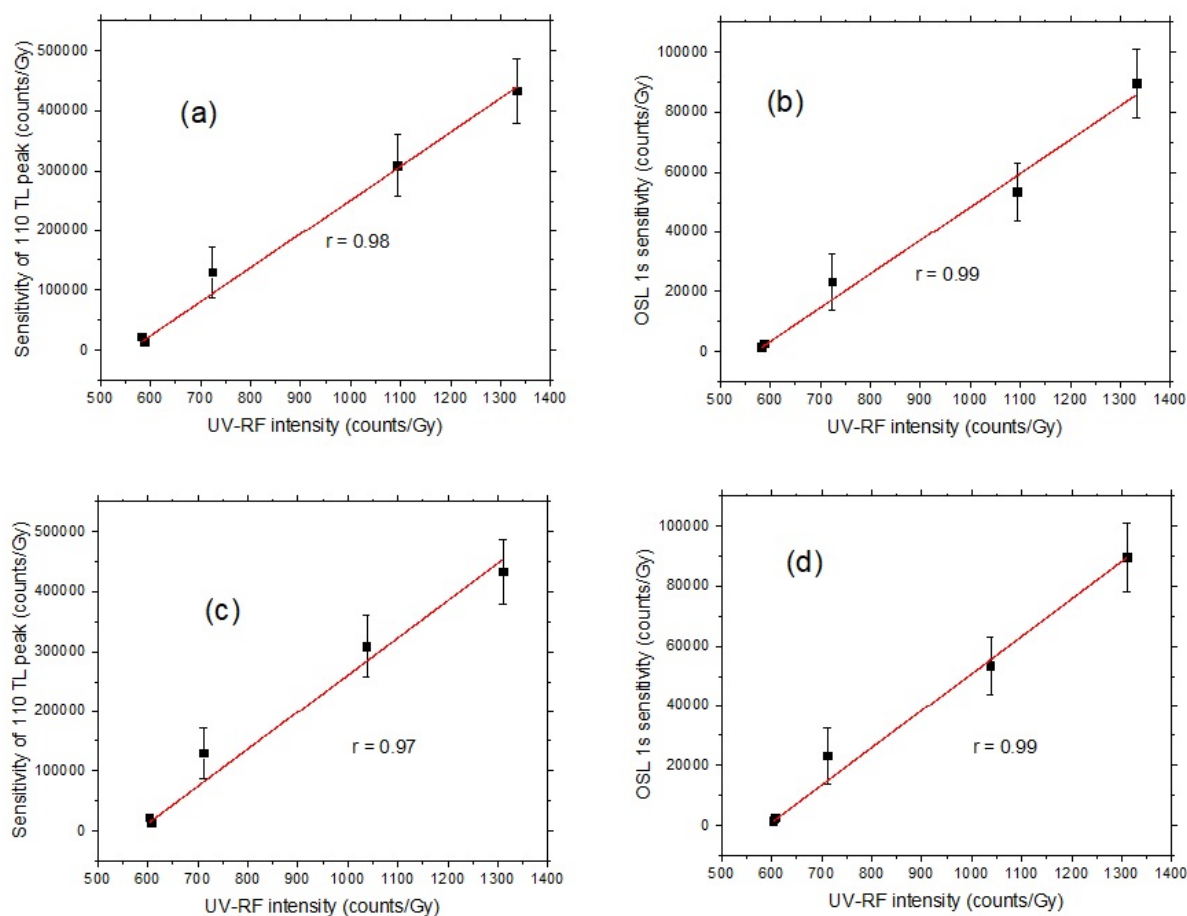


Figure 5. Correlation between 3.6 eV RF emission intensity and the 110 °C TL peak (a) and OSL (b) sensitivities of quartz from sediments. The intensity of the 3.36 eV emission band was also plotted for comparison with the 110 °C TL peak (c) and of OSL (d) sensitivities. The data for all graphs were fitted with a linear equation. For the UV-RF measurement, we only measured one aliquot for each sample.

mainly in the UV and blue emission bands (320–400 nm). However, quartz from sediments recently released from their parent rocks in active tectonic settings (L0017 and L0698) have RF intensity in the same range of quartz from rocks. Additional studies are needed to confirm that a single natural process is promoting the sensitization of quartz TL, OSL, and RF.

In conclusion, the results of this study indicate that quartz RF intensity mirrors sensitivity patterns observed for OSL and TL signals in nature and the UV-RF intensity measured using X-ray sources can also be used for provenance analysis of sediments in the same way as the OSL and TL sensitivities.

Acknowledgments

We appreciate the thoughtful and detailed comments and suggestions by Dr. Sebastian Kreutzer, who greatly contributed to improving the quality of our work. PN is grateful to the National Council for Science and Technology Development (CNPq), The World Academy of Sciences (TWAS)

(CNPq/TWAS grant 154507/2017-2), and The São Paulo Research Foundation (FAPESP grant 2019/04059-6) for funding the Ph.D. fellowship at the University of São Paulo. AOS is supported by the National Council for Science and Technology Development (CNPq grant 304727/2017-2).

References

- Aitken, M. J. *An introduction to optical dating: the dating of quaternary sediments by the use of photon-stimulated luminescence*. Oxford University Press, 1998.
- Aitken, M. J. and Smith, B. M. *Optical dating: Recuperation after bleaching*. *Quaternary Science Reviews*, 7: 387–393, 1988.
- Chen, G., Li, S. H., and Murray, A. S. *Study of the 110 °C TL peak sensitivity in optical dating of quartz*. *Radiation Measurements*, 32: 641–645, 2000.
- Chithambo, M. and Niyonzima, P. *Radioluminescence of annealed synthetic quartz*. *Radiation Measurements*, 106: 35–39, 2017.

- Chithambo, M. L., Preusser, F., Ramseyer, K., and Ogundare, F. O. *Time-resolved luminescence of low sensitivity quartz from crystalline rocks*. *Radiation Measurements*, 42: 205–212, 2007.
- Fleming, S. J. *Thermoluminescence dating: refinement of the quartz inclusion method*. *Archaeometry*, 12: 133–145, 1970.
- Friedrich, J., Fasoli, M., Kreutzer, S., and Schmidt, C. *The basic principles of quartz radiofluorescence dynamics in the UV - analytical, numerical and experimental results*. *Journal of Luminescence*, 192: 940–948, 2017.
- Gray, H. J., Jain, M., Sawakuchi, A. O., Mahan, S. A., and Tucker, G. E. *Luminescence as a sediment tracer and provenance tool*. *Reviews of Geophysics*, 57: 987–1017, 2019.
- Grögler, N., Houtermans, F. G., and Stauffer, H. *Radiation damage as a research tool for geology and prehistory*. In *Convengo sulle dotazioni con metodi nucleari. th Internazation Elettr Nucl Sezione Nuclear Roma*, pp. 5–15, 1958.
- Guralnik, B., Ankjærgaard, C., Jain, M., Murray, A. S., Müller, A., Wälle, M., and Herman, F. *OSL-thermochronometry using bedrock quartz: A note of caution*. *Quaternary Geochronology*, 25: 37–48, 2015.
- Huntley, D. J., Godfrey, S. D. I., and Thewalt, M. L. W. *Optical dating of sediments*. *Nature*, 313: 105–107, 1985.
- Huntley, D. J., Godfrey-Smith, D. I., and Haskell, E. H. *Light-induced emission spectra from some quartz and feldspars*. *Nuclear Tracks Radiation Measurements*, 18: 127–131, 1991.
- Jain, M., Murray, A. S., and Bøtter-Jensen, L. *Characterization of blue-light stimulated luminescence component in different quartz samples: Implications for dose measurement*. *Radiation Measurements*, 37: 441–449, 2003.
- Krbetschek, M. R. and Trautmann, T. *A spectral radioluminescence study for dating and dosimetry*. *Radiation Measurements*, 32: 853–857, 2000.
- Krbetschek, M. R., Götze, J., Dietrich, A., and Trautmann, T. *Spectral information from minerals relevant for luminescence dating*. *Radiation Measurements*, 27: 695–748, 1997.
- Lü, T. and Sun, J. *Luminescence sensitivities of quartz grains from eolian deposits in northern China and their implications for provenance*. *Quaternary Research*, 76: 181–189, 2011.
- Marazuev, Y. A., Brik, A. B., and Degota, V. Y. *Radioluminescent dosimetry of Alpha - quartz*. *Radiation Measurements*, 24: 565–569, 1995.
- Martini, M., Fasoli, M., and Galli, A. *Quartz OSL emission spectra and the role of $[AlO_4]^{0-}$ recombination centres*. *Radiation Measurements*, 44: 458–461, 2009.
- Martini, M., Fasoli, M., Galli, A., Villa, I., and Guibert, P. *Radioluminescence of synthetic quartz related to alkali ions*. *Journal of Luminescence*, 132: 1030–1036, 2012a.
- Martini, M., Fasoli, M., Villa, I., and Guibert, P. *Radioluminescence of synthetic and natural quartz*. *Radiation Measurements*, 47: 846–850, 2012b.
- Mejhdahl, V. *Thermoluminescence dating: Beta-dose attenuation in quartz grains*. *Archaeometry*, 21: 61–72, 1979.
- Mendes, V. R., Sawakuchi, A. O., Chiessi, C. M., Giannini, P. C. F., Rehfeld, K., and Mulitza, S. *Thermoluminescence and optically stimulated luminescence measured in marine sediments indicate precipitation changes over northeastern Brazil*. *Paleoceanography and Paleoclimatology*, 34, 2019.
- Moska, P. and Murray, A. S. *Stability of the quartz fast-component in insensitive samples*. *Radiation Measurements*, 41: 878–885, 2006.
- Nian, X., Zhang, W., Qiu, F., Qin, J., Wang, Z., Sun, Q., Chen, J., Chen, Z., and Liu, N. *Luminescence characteristics of quartz from Holocene delta deposits of the Yangtze River and their provenance implications*. *Quaternary Geochronology*, 49: 131–137, 2019.
- Pietsch, T. J., Olley, J. M., and Nanson, G. C. *Fluvial transport as a natural luminescence sensitizer of quartz*. *Quaternary Geochronology*, 3: 365–391, 2008.
- Prasad, A. K., Lapp, T., Kook, M., and Jain, M. *Probing luminescence centers in Na rich feldspar*. *Radiation Measurements*, 90: 292–297, 2016.
- Rink, W. J., Rendell, H., Marseglia, E. A., Luff, B. J., and Townsend, P. D. *Thermoluminescence Spectra of Igneous Quartz and Hydrothermal Vein Quartz*. *Physics and Chemistry of Minerals*, 20: 353–361, 1993.
- Sawakuchi, A. O., Blair, M. W., DeWitt, R., Faleiros, F. M., Hypolito, T., and Guedes, C. C. F. *Thermal history versus sedimentary history: OSL sensitivity of quartz grains extracted from rocks and sediments*. *Quaternary Geochronology*, 6: 261–272, 2011.
- Sawakuchi, A. O., Guedes, C. C. F., Dewitt, R., Giannini, P. C. F., Blair, M. W., and Faleiros, F. M. *Quartz OSL sensitivity as a proxy for storm activity on the southern Brazilian coast during the Late Holocene*. *Quaternary Geochronology*, 13: 92–102, 2012.
- Sawakuchi, A. O., Jain, M., Mineli, T. D., Nogueira, L., Jr, B., J., D., Häggi, C., Sawakuchi, H. O., Pupim, F. N., Grohmann, C. H., Chiessi, C. M., c, M. Z., Mulitza, S., Mazoca, C. E. M., and Cunha, D. F. *Luminescence of quartz and feldspar fingerprints provenance and correlates with the source area denudation in the Amazon River basin*. *Earth and Planetary Science Letters*, 492: 152–162, 2018.
- Sawakuchi, A. O., Rodrigues, F. C. G., Mineli, T. D., Mendes, V. R., Melo, D. B., Chiessi, C. M., and Giannini, P. *Optically stimulated luminescence sensitivity of quartz for provenance analysis*. *Methods and Protocols*, 3: 6, 2020. doi: <https://doi.org/10.3390/mps3010006>.
- Schilles, T., Poolton, N. R. J., Bulur, E., Bøtter-Jensen, L., Murray, A. S., Smith, G. M., Riedi, P. C., and Wagner, G. A. *A multi-spectroscopic study of luminescence sensitivity changes in natural quartz induced by high-temperature annealing*. *Journal of Physics D: Applied Physics*, 34: 722–731, 2001.
- Schmidt, C., Kreutzer, S., DeWitt, R., and Fuchs, M. *Radiofluorescence of quartz: A review*. *Quaternary Geochronology*, 27: 66–77, 2015.

Shimizu, N., Mitamura, N., Takeuchi, A., and Hashimoto, T. *Dependence of radioluminescence on TL-properties in natural quartz*. *Radiation Measurements*, 41: 831–835, 2006.

Tsukamoto, S., Nagashima, K., Murray, A. S., and Tada, R. *Variations in OSL components of quartz from Japan sea sediments and the possibility of reconstructing provenance*. *Quaternary International*, 234: 182–189, 2011.

Wintle, A. G. and Huntley, D. J. *Thermoluminescence dating of deep sea sediments*. *Nature*, 279: 710–712, 1979.

Zular, A., Sawakuchi, A. O., Guedes, C. C. F., and Giannini, P. C. F. *Attaining provenance proxies from OSL and TL sensitivities: coupling with grain size and heavy minerals data from southern Brazilian coastal sediments*. *Radiation Measurements*, 81: 39–45, 2015.

Reviewer

Sebastian Kreutzer